JOURNAL OF GEOPHYSICAL RESEARCH, VOL. 107, NO. E10, 5088, doi:10.1029/2002JE001891, 2002

# Geologic setting and origin of Terra Meridiani hematite deposit on Mars

Brian M. Hynek, Raymond E. Arvidson, and Roger J. Phillips

Earth and Planetary Sciences and McDonnell Center for the Space Sciences, Washington University, St. Louis, Missouri, USA

Received 23 February 2002; revised 1 June 2002; accepted 25 June 2002; published 25 October 2002.

[1] We have completed a regional analysis of the hematite deposit in Terra Meridiani and conclude that the unit is in the midst of a 600-m-thick stack of friable layered materials superposed on Middle and Late Noachian cratered terrain. The deposits resemble terrestrial pyroclastics in the fact that they are: (1) thin, parallel bedded deposits that conform to preexisting topography, (2) often extremely friable, and (3) composed of fine particles. Some of the lowermost layered units exhibit possible lava flow textures and features. Abundant outliers indicate that the deposits were once far more extensive and that erosion (primarily aeolian) has removed vast portions of the stratigraphic sequence. The hematite may have formed from thermal oxidation of the volcanic ash during eruption or have been precipitated from the circulation of fluids within the layered materials at a later time. Temporal and spatial association with outflow channels and evidence for cementation along joints and bedding planes within the layered deposits suggest the latter scenario. *INDEX TERMS:* 6225 Planetology: Solar System Objects: Mars; 3665 Mineralogy and Petrology: Mineral occurrences and deposits; 5415 Planetology: Solid Surface Planets: Erosion and weathering; 5480 Planetology: Solid Surface Planets: Volcanism (8450); *KEYWORDS:* Mars, Terra Meridiani, hematite, iron, layered

**Citation:** Hynek, B. M., R. E. Arvidson, and R. J. Phillips, Geologic setting and origin of Terra Meridiani hematite deposit on Mars, *J. Geophys. Res.*, *107*(E10), 5088, doi:10.1029/2002JE001891, 2002.

## 1. Introduction

[2] One of the key discoveries from the Mars Global Surveyor (MGS) Mission has been the detection of the mineral hematite by the Thermal Emission Spectrometer (TES) team [*Christensen et al.*, 2000]. The hematite occurs in one primary locale, known as Terra Meridiani (TM) (lat. 3°S–1°N, lon. 352°E across the prime meridian to 1°E; covering $\sim 9 \times 10^4$ km$^2$), with minor occurrences in Aram Chaos and Valles Marineris (Figure 1). *Christensen et al.* [2000, 2001] characterized the Terra Meridiani deposit as primarily andesitic–basaltic sediments with 10 to 15% (areal abundance) of crystalline, gray, coarse-grained (>5–10 μm) hematite. *Lane et al.* [2002] showed evidence for platy hematite and suggested that deposits underwent burial metamorphism and since have been exhumed.

[3] Deposits of layered materials have been recognized in the TM area since the late-1970s and numerous mechanisms for their origin were proposed based on Viking imagery and thermal data. *Scott and Tanaka* [1986] and *Presley and Arvidson* [1988] described the materials as friable sediments that likely consisted of aeolian deposits decoupled from the underlying bedrock. *Schultz and Lutz* [1988] argued that TM units were part of a global set of antipodal equatorial layered materials that they proposed were ancient polar deposits, indicative of true polar wandering in the past. Alternatively, *Edgett and Parker* [1997] hypothesized that TM units accumulated in an ancient subaqueous environment. The analysis of Mars Orbiter Camera (MOC) data led *Malin and Edgett* [2001] to suggest that the materials are not sedimentary mantling units but are bedrock outcrops of the ancient Martian crust.

[4] The discovery of crystalline gray hematite, or specularite ($Fe_2O_3$), on Mars has created a renewed interest in TM and its deposits. On Earth, hematite forms in numerous ways, and most require liquid water. For example, terrestrial Archean Banded Iron Formations (BIF) likely formed in a subaqueous environment [e.g., *Guilbert and Park*, 1986]. *Hitzman et al.* [1992] argued for the formation of crystalline hematite as a precipitate from circulating Fe-rich hydrothermal fluids in Proterozoic iron oxide deposits. Low-temperature dissolution and precipitation from groundwater (leaching) has formed expansive terrestrial laterites and ferricretes rich in hematite [*McFarlane*, 1976]. Additionally, hematite is commonly found as a surface coating that is a result of the interaction between Fe-rich rocks and surface or atmospheric water [*Guilbert and Park*, 1986]. However, the formation of gray crystalline hematite on Earth does not always require liquid water. The eruption of Fe-rich lavas have resulted in large hematite-rich ash flows and falls around Cerro de Mercado, Mexico [*Lyons and Clabaugh*, 1973; *Swanson et al.*, 1978] and almost pure magnetite-


0148-0227/02/2002JE001891$09.00

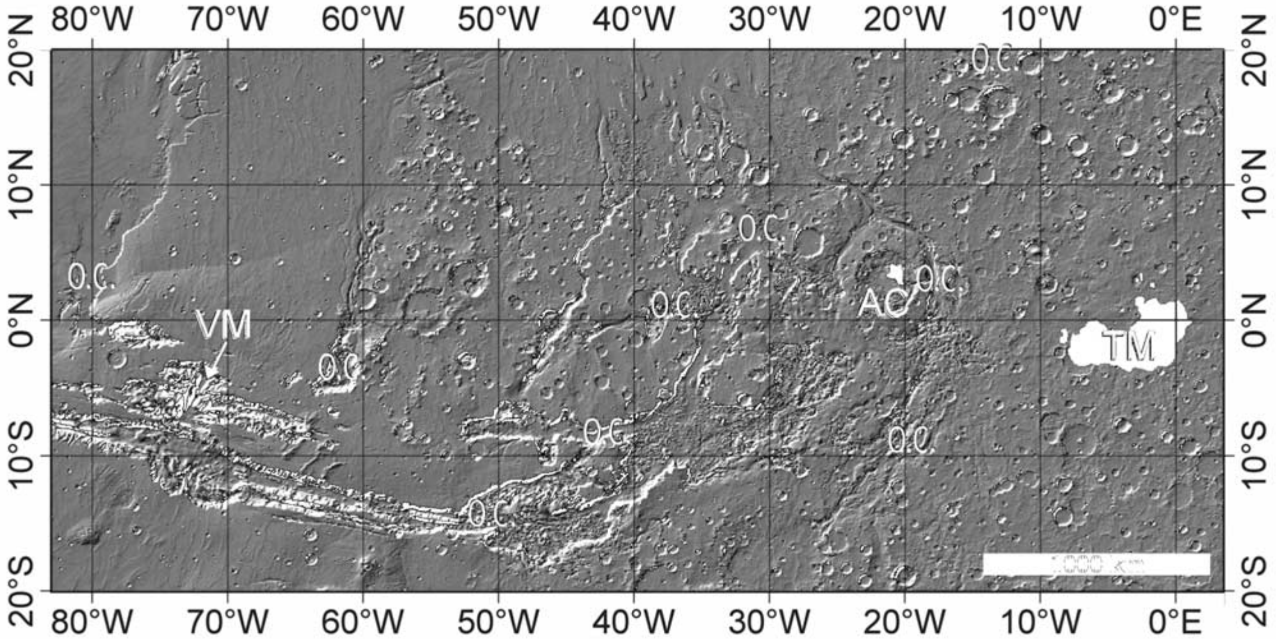


**Figure 1.** Regional view of the three hematite locales. MOLA shaded relief map used as base with hematite index overlain. Terra Meridiani = TM, Aram Chaos = AC, Valles Marineris = VM. Some TES data taken from *Christensen et al.* [2001]. An abundance of martian outflow channels (labeled O.C.) occur in close proximity to the hematite, suggesting an association with subsurface fluids. Coordinate system is MOLA-defined planetocentric.

hematite lava flows in El Laco, Chile [*Park*, 1961; *Rogers*, 1968; *Nyström and Henríquez*, 1994]. *Christensen et al.* [2000, 2001] examined the above formation mechanisms and their viability in the Martian environment. Association with layered deposits and a strong correlation with geologic units led them to favor precipitation from Fe-rich water, either in a low-temperature subaqueous environment or a hydrothermal system.

[5] Understanding the origin of Martian hematite is essential for unraveling the geologic, aqueous, and possibly the climatic histories of the TM region of Mars. All of the above "wet" hypotheses require the availability of liquid water at or near the surface of Mars for an extended period of time. Hence, TM deposits have quickly emerged as a primary target for near-future exploration of Mars. If indeed the hematite has a "wet" origin then the possibility of initiation, and even preservation, of prebiotic or biotic processes exists [*Allen et al.*, 2001]. In this paper we present a detailed geologic study of the principal Martian hematite deposit that places it in a regional geologic context. This approach allows us to scrutinize the diverse origin mechanisms of hematite.

## 2. Characterization of the Terra Meridiani Deposits

### 2.1. Geomorphic Mapping Methods

[6] Detailed geomorphic mapping of Terra Meridiani (lat. 5°S to 10°N, lon. 12°W across the prime meridian to 5°E) has been completed at 1:1,000,000 scale using Viking Mars Digital Image Mosaic (MDIM 1) as a base that was converted to the planetocentric MOLA-defined coordinate system (Figure 2). This latitude and longitude range includes the primary hematite deposit and associated layered deposits, although there is evidence that these materials once had a much greater extent (section 3). We have incorporated available data from MGS including fine-scale (64 pixels/degree latitude, 32 pixels/degree longitude) topographic grids from the Mars Orbiter Laser Altimeter (MOLA), individual topographic profiles, corrected MOLA pulse width (a measure of surface roughness at MOLA laser wavelength scale), over 100 MOC narrow- and wide-angle (NA and WA) images, TES spectra, and TES-derived albedo and thermal inertia. Many of the units have likely undergone advanced degrees of erosion and some may even be exhumed surfaces [*Lane et al.*, 2002]. This observation constituted geomorphic (rather than geologic) mapping, although lithostratigraphic properties (e.g., spectral signature and other TES- and MOLA-derived data sets) were implemented when possible. MOLA data have been used to constrain the thickness of units, characterize their slopes and surface roughness, and to test for lateral continuity across the mapped area.

### 2.2. Major Terrain Types

[7] It has become clear that the type hematite locale within Terra Meridiani is not an isolated deposit; rather, it is one stratum in the midst of a thick (~600 m of relief) layered sequence of deposits that buries tilted Noachian cratered terrain [*Hynek et al.*, 2001]. Portions of the sequence are seen for hundreds of kilometers and bedding remains remarkably horizontal to subhorizontal and uniform. The deposits are believed to consist of coarse sand comprising layers of varying competency, which may reflect differing degrees of induration within layers. The

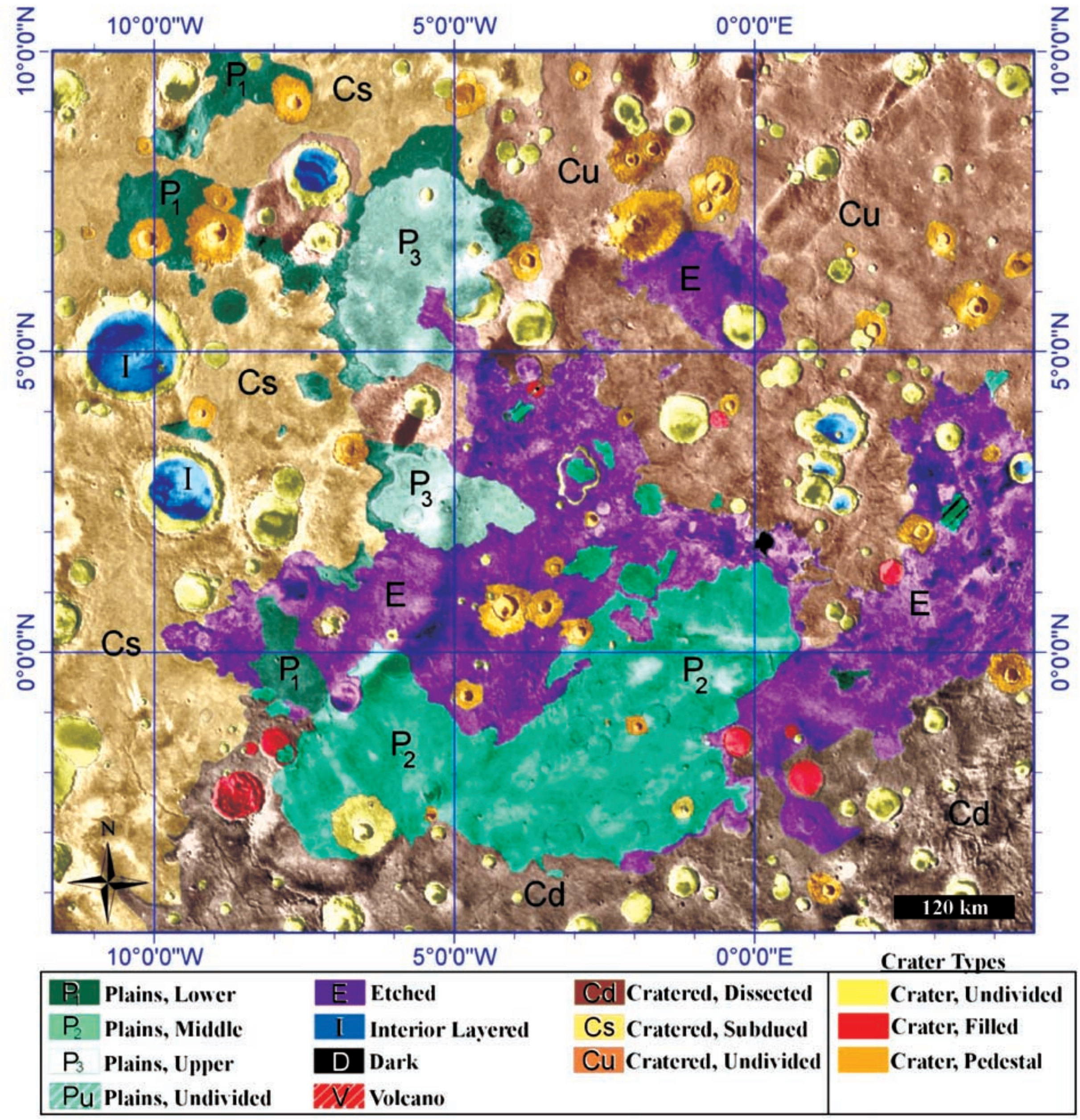


**Figure 2.** Geomorphic map of Terra Meridiani showing terrain units and distribution of crater types. The hematite ($P_2$) is in the midst of a complex stratigraphic sequence of layered materials. These younger layered deposits ($P_1$, $P_2$, $P_3$, E, I) are superposed on ancient cratered terrain and have numerous outliers in the western region of the mapped area. This observation and the abundance of pedestal craters suggest that the layered materials once had a much greater extent (see section 3).

small clast size is inferred from thermal conductivity studies [*Presley and Christensen*, 1997] and TES data [*Jakosky and Mellon*, 2001] and the observation that sand dunes, and not boulders, are seen at the eroded edges of the deposits. Outliers have eroded into yardang-like shapes and also lack boulders greater than 2–3 m in size (pixel resolution of MOC) (Figure 3A). Their thinly layered nature indicates that the TM deposits were emplaced episodically over an unknown time period. The mantling deposits have been divided into several plains units ($P_1$, $P_2$, $P_3$) and a single etched unit (E) consisting of numerous deposits stratigraphically between and below the plains units that have experienced a severe degree of erosion, rendering the correlation of individual layers impossible. Figure 3 shows MOLA elevation overlain on a Viking MDIM and illustrates the typical surface features of these units at MOC resolution while placing results in a regional context. The layered deposits clearly bury the underlying cratered terrain and thus indicate a differing lithology and younger age, in contrast to the conclusion reached by *Malin and Edgett* [2001]. Valley networks on the sloping, older, cratered unit are buried along the contact with the layered deposits in

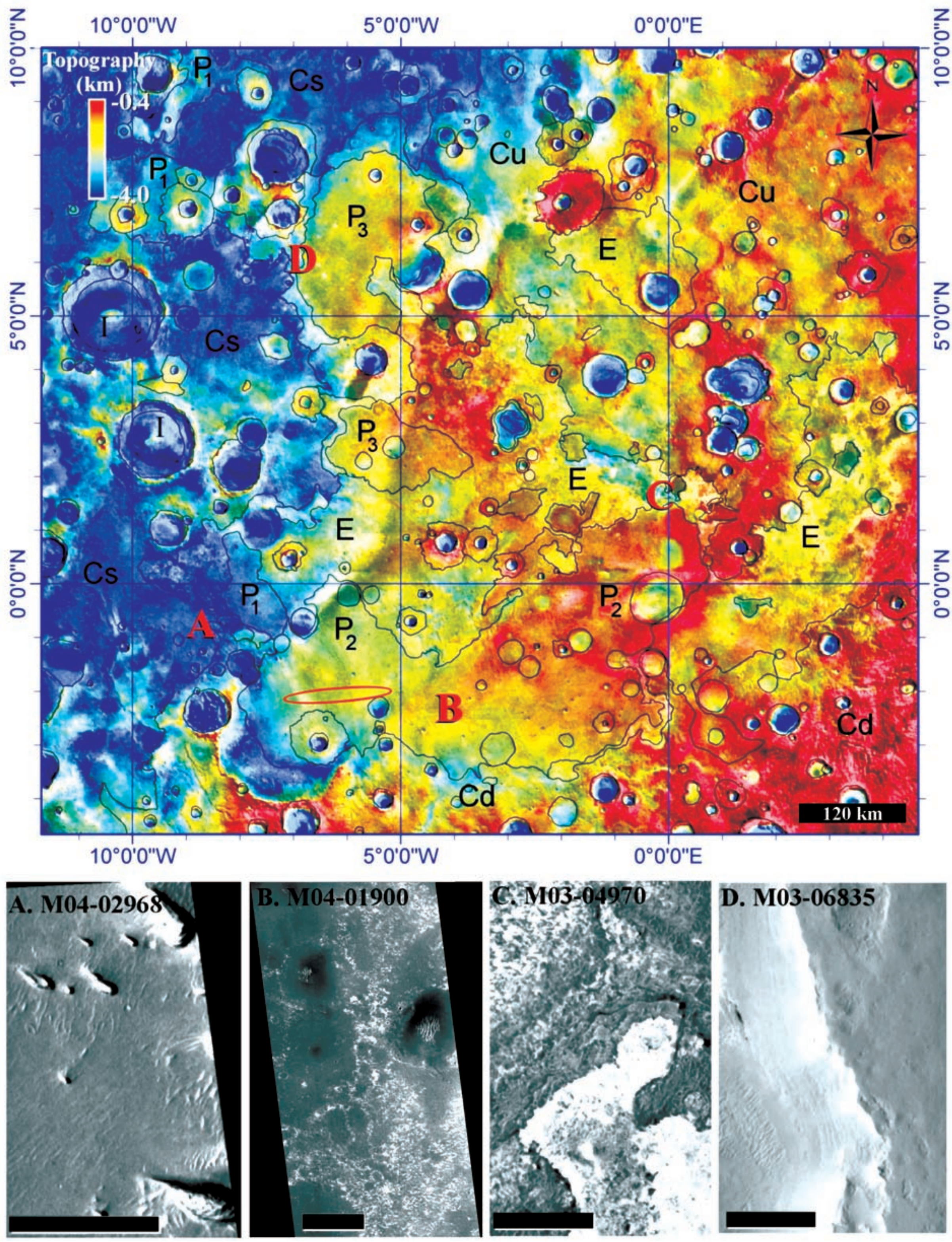


**Figure 3.** MOLA-derived topography of Terra Meridiani region with outlines of geomorphic units overlain on Viking MDIM 1 warped into the MOLA-defined coordinate system (unit key in Figure 2). Red ellipse indicates the proposed landing site for the 2003 Mars Exploration Rovers (MER) Mission [*Golombek et al.*, 2002]. (A–D) Illustrate the typical surface features of key geomorphic units at MOC NA resolution while placing them in a regional context. Note the superposition of the Terra Meridiani deposits with the older valley networks and cratered terrain. The scale bar on each MOC image is 1 km and all MOC images in this paper are in a sinusoidal projection with north toward the top of image.

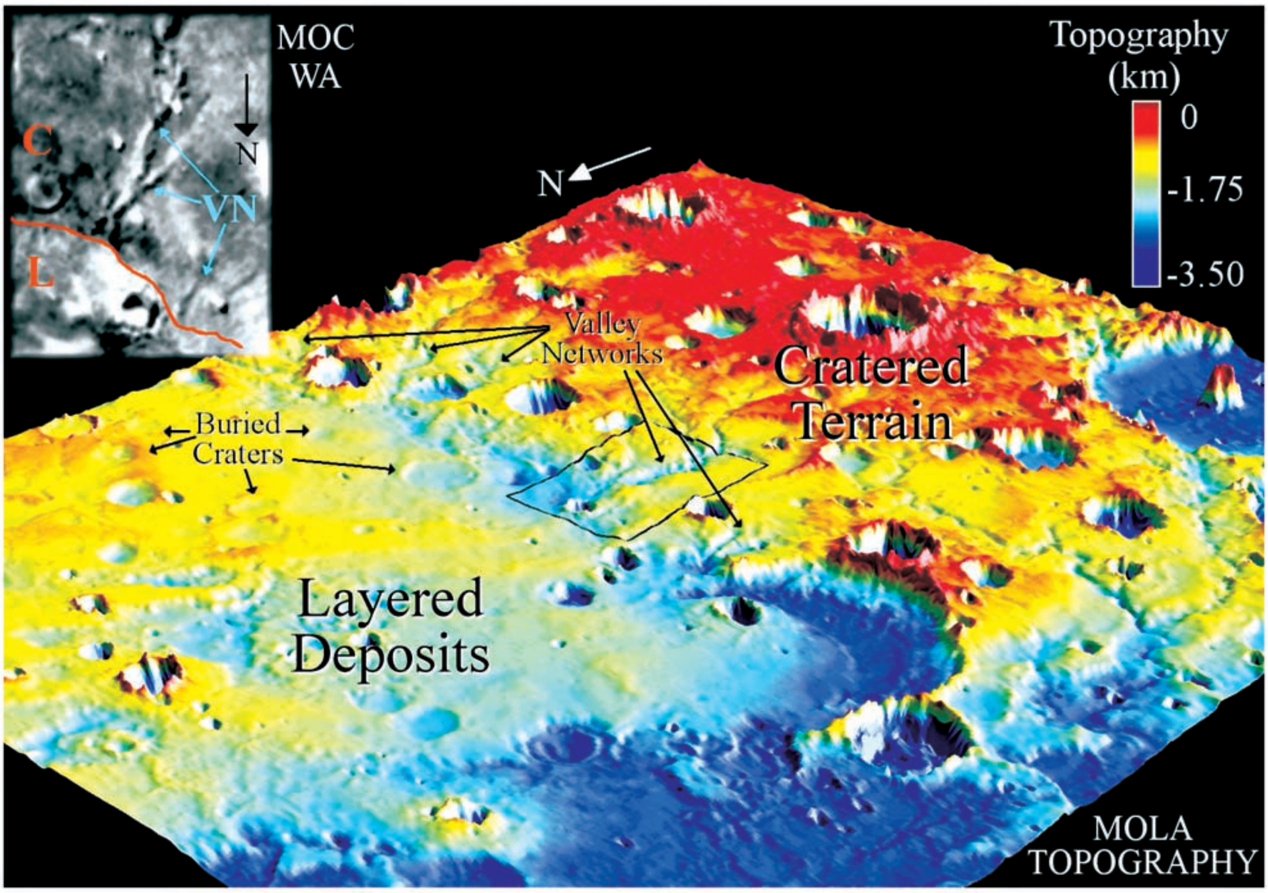


**Figure 4.** Oblique view of a MOLA shaded relief image of Terra Meridiani with a color scheme overlain. The extent is 2°N–10°S and 0–10°W and the line of sight is southeast. The layered deposits of Terra Meridiani are seen in the north half of the view, superposed on the sloping cratered terrain to the south. Valley networks on the cratered material end abruptly at the contact with the younger layered deposits, which also buries craters that are presumably part of the underlying cratered terrain. Inset is a MOC WA mosaic taken from the black box on large view. Image illustrates the contact (orange line) between the dissected cratered unit (C) and the younger layered material (L). The figure corroborates topographic evidence for burial of valley networks along the geologic contact, indicating that the layered deposits are younger and geologically distinct from the cratered material. Vertical exaggeration is 25×.

MOLA and MOC data (Figure 4). Moreover, the subdued rims of underlying craters from the older terrain are seen in high-resolution topography of the mantling materials.

**2.2.1. Description of Map Units**

[8] *Plains Units* ($P_1$, $P_2$, $P_3$)—Smooth, laterally extensive, thick (~600 m) layered sequence of plains units. Stratigraphic sections of the layered sequence are seen for thousands of square kilometers and the bedding remains remarkably consistent and uniform over these distance scales. Plains units mantle underlying topography as well as abut highstanding, steep-sided inliers of older cratered terrain. All plains units exhibit some degree of aeolian erosion, particularly on their fringes. Numerous outliers suggest that these units were once much more extensive (section 3, Figures 2 and 3A). Three competent plains units are distinguishable and abridged descriptions of them follow:

1. $P_3$—Consists of smooth (at Viking scale), massive (~200 m thick), relatively high albedo, cliff-forming plains material (Figure 3D). Individual layers are not observed although current MOC NA coverage of this unit is sparse and unit appears mantled by dust.

2. $P_2$—Dark, smooth plains (at Viking, MOC, and MOLA pulse width scales) composed of resistant layered material (Figure 3B) with low thermal inertia [*Arvidson et al.*, 2002] and thickness of less than a few hundred meters. Small mesas and underlying bright terrain can be seen in some MOC NA images of the unit, indicating that the surface may be exhumed. Unit is similar in morphology, elevation, and erosional characteristics (at Viking scales) to $P_3$, although TES data indicate that this unit is compositionally rich in hematite (~10–15%) [*Christensen et al.*, 2000] and has a distinct thermal inertia and albedo [*Arvidson et al.*, 2002].

3. $P_1$—Thick (~200 m), resistant unit with some layering comprises lowermost portion of plains materials. Numerous outliers exist and occur at the same elevation, indicating that the unit once had a greater areal coverage (Figure 2).

[9] *Etched Unit* (E)—Indurated deposits with high thermal inertia [*Arvidson et al.*, 2002] that are stratigraphically below upper plains members ($P_2$, $P_3$) and above and below

**Table 1.** Properties of Major Terrain Units for the Terra Meridiani Region, Mars (Figure 2)

| Unit Name | Unit Symbol | Area, $km^2$ | Minimum Elevation,[a] m | Maximum Elevation,[a] m | Mean Elevation, m | $N(5)$ Age[b] | $N(16)$ Age[b] | Relative Upper Age Limit[c] | Likely Age[d] |
|---|---|---|---|---|---|---|---|---|---|
| Plains, Upper | $P_3$ | 31,843 | −2357 | −896 | −1388 | 220 ± 83 | 94 ± 54 | MN–EH | LN–EH |
| Plains, Middle | $P_2$ | 88,670 | −3002 | −1020 | −1361 | 226 ± 50 | 135 ± 39 | MN–EH | LN–EH |
| Plains, Lower | $P_1$ | 33,976 | −2743 | −1127 | −1692 | 206 ± 78 | 29 ± 29 | LN–EH | LN–EH |
| Etched | E | 146,808 | −2884 | −668 | −1364 | 272 ± 43 | 102 ± 26 | MN–LN | LN–EH |
| Interior Layered Crater | I | 11,243 | −3586 | −1198 | −2614 | 267 ± 154 | 267 ± 154 | EN–LH | LN–EH |
| Cratered, Subdued | Cs | 193,443 | −3982 | −1001 | −1902 | 295 ± 39 | 114 ± 24 | MN–LN | MN–LN |
| Cratered, Dissected | Cd | 139,676 | −2918 | −51 | −1263 | 437 ± 56 | 179 ± 36 | EN–LN | MN–LN |
| Cratered, Undivided | Cu | 238,950 | −3370 | −545 | −1384 | 423 ± 42 | 151 ± 25 | MN–LN | MN–LN |

[a] Thickness is not reflected in the difference between minimum and maximum elevations because many of these areally extensive deposits were emplaced on a preexisting regional tilt.

[b] Average total crater density $N(D)$ equals the number of craters larger than diameter $D$ per million square kilometers. Error values were calculated by assuming a Poisson distribution, allowing $1\sigma$ to be estimated as $N = \pm (N)^{1/2}$, where $N$ is the number of craters [*Arvidson et al.*, 1979].

[c] Relative upper age limits are given. Variance is from $N(5)$ and $N(16)$ ages and calculated errors. E = Early, M = Middle, L = Late, N = Noachian, H = Hesperian. Many craters included in the layered materials ($P_1$, $P_2$, $P_3$, E, I) are partially buried, filled, or mantled and probably represent underlying cratered terrain (Cs, Cd, or Cu). Additionally, these numbers are based only on total crater counts since superposed counts were statistically invalid on all units due to very few fresh craters and small areal extent of units. See discussion in section 2.3.

[d] Probable ages are given and include relative ages from crater densities as well as mapping relationships from this study and *Hynek and Phillips* [2001].

the lowermost plains unit ($P_1$). The unit contains many strata that have undergone differential erosion to form ridges, mesas, pits, and troughs with relief up to hundreds of meters (Figure 3C). Several of these layers contain evidence for local reworking of material, including possible cemented dune fields.

[10] *Interior Layered Crater Deposits* (I)—Exist as thinly layered mounds of friable material superposed within impact basins on the cratered terrain (Cs, Cd, Cu). The stacks are generally near the central region of craters and sometimes are topographically higher than the rim. It is unclear whether these are outliers of the plains and etched units ($P_1$, $P_2$, $P_3$, E), although their proximity, similar bedding morphology, and erosional characteristics suggest that there might be an intimate stratigraphic relationship.

[11] *Cratered, Subdued* (Cs)—Heavily cratered unit composed of large degraded impact basins and smooth intervening deposits. The unit is likely a vestige of a Late Noachian denudation event that removed vast volumes of cratered highland material in this region [*Hynek and Phillips*, 2001]. Many crater rims appear to be subdued, partly removed, or buried. Crater floors are smooth and generally do not have central peaks. At MOC WA and NA scale, numerous outliers of the plains and etched terrains ($P_1$, $P_2$, $P_3$, E) are superposed on the unit in wind-eroded forms (Figures 2 and 3A). Unit is similar to *Npl*$_2$, as described on the 1:15,000,000 scale map by *Scott and Tanaka* [1986].

[12] *Cratered, Dissected* (Cd)—Rugged, low albedo, densely cratered material that is highly dissected by valley networks. Previously mapped as Late Noachian in age and likely correlated to a major erosional event during this era [*Hynek and Phillips*, 2001]. Unit is similar to Npld, as described on the 1:15,000,000 scale Western hemisphere map by *Scott and Tanaka* [1986].

[13] *Cratered, Undivided* (Cu)—Rough cratered terrain with prominent, yet degraded, craters and rim material. Unit is similar to *Npl*$_1$, as described on the 1:15,000,000 scale Western hemisphere map by *Scott and Tanaka* [1986].

[14] *Malin and Edgett* [2001] recently argued that the plains materials are not superposed on the cratered highlands; rather they are outcrops of the ancient terrain. Our mapping substantiates the idea that the layered sequence is superposed on the cratered terrain and therefore is younger (Figures 2, 3, and 4). Additionally, crater counts of the surrounding terrain and the layered units indicate two distinct ages (see below, Table 1). Our results contend that the plains and etched units ($P_1$, $P_2$, $P_3$, E) are geologically distinct from the underlying and surrounding cratered terrain, consistent with previous studies [*Scott and Tanaka*, 1986; *Presley*, 1986; *Presley and Arvidson*, 1988; *Schultz and Lutz*, 1988; *Edgett and Parker*, 1997; *Christensen et al.*, 2000, 2001; *Hynek and Phillips*, 2001; *Hynek et al.*, 2001].

### 2.3. Age Constraints on the Terra Meridiani Materials

[15] Stratigraphic relations from mapping and Viking-based crater counts (Table 1) have allowed us to correlate map units and devise a relative geologic history. However, the extreme degree of erosion that the units have experienced and the possibility that some, or even many, of the units represent exhumed surfaces prohibits the accurate conversion to an absolute timescale in many cases. Crater counts were completed following the method of *Tanaka* [1986] and incorporating the Viking crater database produced by *Barlow* [1988] (Table 1). Our geomorphic map was converted to a geographical information system (GIS) format for statistical and comparative analyses. Areas and crater size-frequency distributions were determined for each individual polygon (mapped exposure) and the geomorphic unit as a whole. Crater statistics were used to create cumulative size-frequency plots for each unit. We applied results from the standard 5 and 16 km frequency distributions for each unit to the absolute timescale by *Hartmann and Neukum* [2001].

Results indicate that all three cratered units (Cs, Cd, Cu) probably formed in the Middle to Late Noachian epoch, toward the end of heavy bombardment (Table 1). These units likely retain enough large diameter craters to devise plausible production ages. Even if these surfaces were subsequently buried, this would have occurred after the sharp drop in the influx of big impactors (since the units that directly overlie have few large craters). Thus, crater dating techniques may be useful in deriving an accurate age range for the cratered units.

[16] It is unlikely that the stratigraphically younger plains ($P_1$, $P_2$, $P_3$), etched (E), and interior layered cratered (I) materials have meaningful crater production or retention curves. *Lane et al.* [2002] suggested that burial, metamorphism, and exhumation of TM could produce platy hematite grains that could explain the hematite c-face dominated spectral signature seen in TES spectra. Our mapping substantiates the notion of burial and exhumation, as argued below; although it remains unclear if the hematite was ever at a sufficient depth and/or high enough temperatures for burial metamorphism to occur [*Lane et al.*, 2002]. Since the hematite and associated layered sequence are superposed on all three Middle to Late Noachian cratered units, an upper bound on their age is Late Noachian ($\sim$3.7 Ga [*Hartmann and Neukum*, 2001]). Counts of superposed craters (those with discernible ejecta; and therefore younger than the unit) translate to a lower age limit of Late Amazonian for all the plains and etched unit although burial and/or modification of these surfaces may be responsible for an unrealistically young age limit that represents the age of modification as opposed to the actual emplacement. The small areal extent of some geomorphic units introduces additional statistical uncertainties.

[17] Counts of total (with or without ejecta) cumulative craters with diameters less than or equal to 5 km and 16 km indicate that the plains and etched units ($P_1$, $P_2$, $P_3$, E) have a probable age of Late Noachian to Early Hesperian (Table 1). Alternatively, *Hartmann et al.* [2001] suggested that quasi-circular depressions seen in MOC images in the hematite-rich unit may be evidence of fossil craters (Figure 3B). If these shallow depressions are fossil craters, in some MOC frames their frequency distribution nears the saturation limit for Mars, suggesting the materials formed during the heavy bombardment era [*Hartmann et al.*, 2001]. However, within a single MOC frame, the proposed fossil craters may be near crater saturation in one region and completely void of craters just a few kilometers away with the surface remaining a constant elevation (e.g., M04-01900, M08-08066, E03-00624, E05-02642). This non-random distribution would suggest obliteration or burial in selected areas although there is little evidence of this in the MOC frames. Additionally, the associated layered units ($P_3$, $P_1$, E) occurring stratigraphically above and below $P_2$ show none of the quasi-circular features in MOC images. As noted above, superposition relationships argue against an Early to Middle Noachian age for the layered sequence. *Chapman and Tanaka* [2002] note the lack of any proposed fossil craters >2 km, an unlikely result because burial or removal should have affected a suite of craters with a range of initial impact diameters. Therefore, it is unlikely that these relatively high albedo ring features are individual fossil craters from the heavy bombardment era and must be explained by another exogenic or endogenic mechanism.

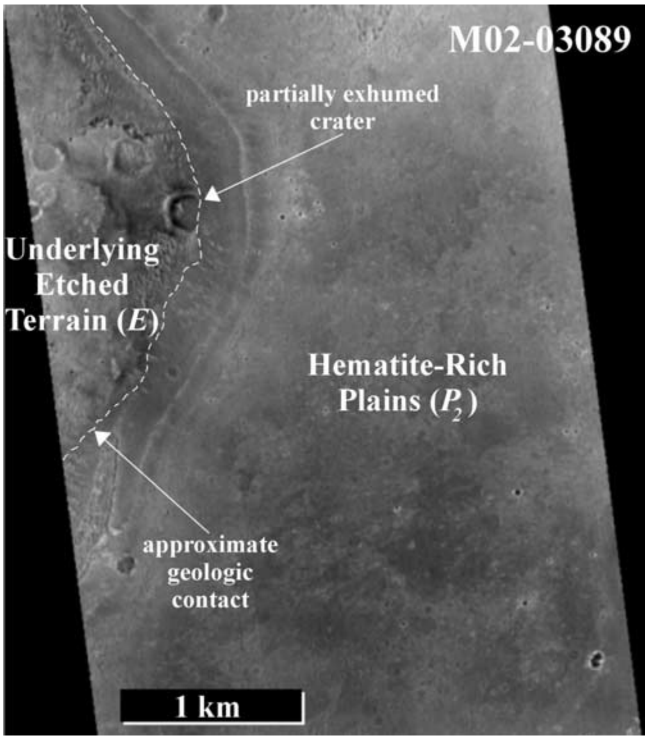


**Figure 5.** MOC NA image showing partially exhumed crater at the contact of the topographically high hematitic plains unit ($P_2$) and the lower etched terrain (E). A lack of boulders along the contact indicates that these units are composed of fine-grained materials.

## 3. Original Extent of the Terra Meridiani Deposits

[18] Thermal data from Viking and MGS reveal that the layered deposits of TM are composed of small grain sizes and are poorly indurated relative to the underlying cratered materials. Wind has been a very effective geomorphic agent in this region, resulting in the erosion and transportation of materials. For example, MOC images show evidence of erosion including the exhumation of craters along the margins of the layered materials (Figure 5). Conversely, the underlying cratered highlands do not appear to be significantly modified by aeolian erosion. The contrasting erosional styles of these two major terrain types in TM are a reflection of their differing lithologies. The younger layered materials are relatively incompetent and have likely undergone significant aeolian erosion. If these materials were emplaced near the Late Noachian/Early Hesperian boundary ($\sim$3.7 Ga [*Hartmann and Neukum*, 2001]), and have been eroded by wind since formation, the original extent of deposits may have been far greater than indicated by the material visible at present.

[19] An abundance of craters containing layered material on their floors occur within the mapped region (Figure 2). Although the occurrence of these deposits has been known

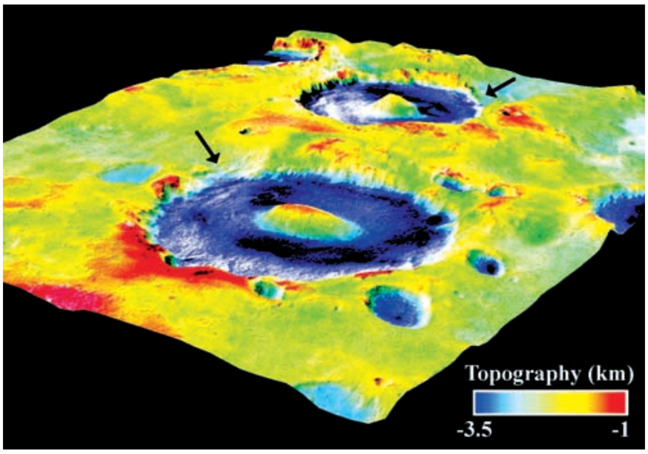


**Figure 6.** Oblique view of two large (>100 km) impact basins in Terra Meridiani with ~2 km-high layered stacks of material in their interior. The deposits are clearly higher than portions of the crater rim (arrows point to examples), making a lacustrine origin unlikely. The interior deposits are probably subaerial in origin and may be part of the same stratigraphic sequence of layered materials that includes the hematite deposit. Vertical exaggeration is 10×.

for years, high-resolution MOC imaging resolved their thinly layered (a few to several hundred meters) strata [*Malin and Edgett*, 2000]. Layered stacks of material are found within many of the larger craters in the surrounding cratered units (Cs, Cd, Cu) (Figure 2). *Malin and Edgett* [2000] indicated that similar sedimentary deposits are found globally, although a majority of the finely layered stacks occurs in craters in and around TM. They argued that the materials within craters might be evidence of lacustrine deposition. However, for most of these deposits there are no associated upgradient source regions, creating a substantial mass balance problem. Additionally, numerous layered stacks are topographically higher than portions of the proposed basin divide (we assume rim topography has not significantly changed since the deposits were formed) (Figure 6). It is also unlikely that these materials are remnants of a hypothesized ocean early in Mars' history [*Edgett and Parker*, 1997] because the deposits rest on a preexisting regional tilt that trends toward the northern plains. If the area was underwater at the time of emplacement of these deposits (and assuming there were no kilometer-scale topography shifts since emplacement) the entire northern third of Mars would have had to been under an ocean that was >4 km deep [*Smith et al.*, 1999]. A subaerial origin of either aeolian and/or volcanic air fall deposits and subsequent exhumation is a more plausible explanation for most of these layered stacks of material. The finely layered stacks are similar in relief, layer thickness, albedo, thermal inertia, spectral signature, and erosional characteristics (high susceptibility to wind-related processes) to the nearby plains ($P_1$, $P_2$, $P_3$) and particularly the etched (E) unit suggesting that they may have a similar origin. It is conceivable that these isolated, layered stacks within craters may have originally been laterally contiguous with the plains and etched terrains ($P_1$, $P_2$, $P_3$, E). If the layered deposits in nearby craters are part of the same lithostratigraphic sequence, the TM deposits originally had a much greater areal extent and have since been eroded to their current coverage. Outliers may be preferentially preserved in craters because rim topography acts as a barrier to surface winds and inhibits transport paths out of the basin. It is even possible that much of the equatorial region of Mars could have at one time been buried by fine-grained, layered sediments to a depth of several kilometers [*Hynek et al.*, 2002]. These workers analyzed MGS data of global equatorial layered deposits and concluded that they are geologically similar and may be a result of explosive volcanism predominately from the Tharsis region. Erosion has been a dominant force in removing much of these materials and has left remnants, including the TM deposits, scattered around the globe.

[20] In the TM region, layered erosional remnants are also seen outside of craters [*Hynek et al.*, 2001]. Numerous circular outlying mesas of the lower plains ($P_1$) occur west of the largest contiguous portions of the unit (Figures 2 and 3). Their relief and morphology indicate that these may be craters and ejecta from the underlying subdued cratered unit (Cs) that were buried by the plains sequence ($P_1$, $P_2$, $P_3$) and have not yet been exhumed. Additionally, MOC images in the subdued cratered unit (Cs) show wind-sculpted layered erosional remnants, providing further evidence that the TM deposits once had a larger areal extent (Figure 3A).

[21] An abundance of pedestal craters in the mapped area also suggests that the TM deposits once had a much greater extent and thickness (Figure 2). Pedestal craters occur in numerous geologic settings on Mars and are identified by a crater and its associated ejecta that are elevated above the surrounding terrain. *Schultz and Lutz* [1988] attributed pedestal craters to impactors that hit a soft mantling deposit. Over time the surrounding friable materials are differentially eroded, leaving only the now topographically high crater and resistant ejecta cap. In the mapped region, pedestal craters have relatively low thermal inertia values when compared to all other craters (typically 100–250 J-m$^{-2}$–s$^{-1/2}$–K$^{-1}$ lower). In fact, their thermal inertias closely resemble that of the surrounding plains ($P_1$, $P_2$, $P_3$) and portions of the etched (E) terrain. These similar values may imply that these craters have substantial amounts of plains ($P_1$, $P_2$, $P_3$) and etched (E) material on their surface, providing evidence of mixing of the preexisting layered deposits in ejecta material. Thus, thermal inertia values may be useful in separating preexisting craters formed on the Noachian-age surfaces (Cs, Cd, Cu) from those that were created after the mantling deposits ($P_1$, $P_2$, $P_3$, E) were emplaced atop the Noachian cratered terrain.

## 4. Hypotheses Regarding Origin of the Terra Meridiani Deposits

### 4.1. Formation of Hematite

[22] *Christensen et al.* [2000, 2001] considered likely formation mechanisms of the hematite deposit and divided these into two major categories: (1) chemical precipitation, subdivided into (a) precipitation from low-temperature subaqueous environment, (b) precipitation from Fe-rich hydrothermal fluids, (c) mobile groundwater leaching, and (d) surface weathering, and (2) thermal oxidation of magnetite-rich volcanics. Some of the above formation mechanisms of hematite could be coeval with the emplacement of the layered materials (primary) while others are secondary

**Table 2.** Consistency of Proposed Hypotheses With Observations and Regional Geomorphic Mapping of the Terra Meridiani Hematite Locale[a]

| Origin | Proposed Hypothesis | Subdivision | Observations of Hematite and Associated Layered Deposits | |
|---|---|---|---|---|
| | | | Consistent | Inconsistent |
| Primary | Precipitation from Fe-Rich Waters | Low-Temperature (i.e., Lake) | smooth, layered, friable deposits of constant thickness | no obvious closed basins; timing of deposits likely after proposed clement period on Mars [*Jakosky and Phillips*, 2001]; no source regions for lacustrine deposits; only one layer of 600 m-thick stratigraphic sequence is hematite-rich; lack of a silica phase (as typically found in Banded Iron Formations on Earth) |
| | | High-Temperature (i.e., Hydrothermal) | possible cemented joint systems and differential erosion within units; spatial and temporal associations with outflow channels | large areal extent ($>10^5$ km$^2$); lack of any associated hydrothermally altered products in TES data; lack of tectonism or obvious heat source |
| | Thermal Oxidation of Volcanic Deposits | Lava Flows | primarily andesitic–basaltic composition; possible volcanic features including small ridge vents, dikes, and flow features | lack of volcanic constructs; martian lavas are generally far less susceptible to erosion than the observed deposits; 600 m-thick sequence with nearly constant layer thickness throughout; paucity of boulders along eroded margins |
| | | Ignimbrites | friable deposits; flat, smooth upper surfaces; highly susceptible to erosion; possible primary volcanic features; fine-grained deposits | lack of volcanic constructs; conform to preexisting topography |
| | | Air Fall | thin bright and dark layers that drape over preexisting topography; highly susceptible to erosion; widespread, fine-grained deposits | lack of nearby sources |
| Secondary | Groundwater Diagenesis | Leaching | possible cemented joint systems and differential erosion within units; large areal extent | red not gray hematite more probable; sharp boundaries and correlation with geomorphology |
| | | Hydrothermal Alteration Along Permeable Layers | one hematitic layer in the midst of a stratigraphic sequence; possible joint systems and differential erosion within units; spatial and temporal associations with outflow channels | lack of any associated hydrothermally altered products in TES data; lack of tectonism or obvious heat source |
| | Coating of Fe-Rich Rock | Surface Weathering | common hematite formation process on Earth | generally produces red, not gray, hematite; platy grains; lack of substantial atmospheric water |

[a] Hydrothermal is listed as both primary and secondary. In the former scenario, hydrothermal activity produces the hematite and the hundreds of meters of associated layered deposits. In the latter case, hematite is hydrothermally precipitated along layers of preexisting Fe-Rich strata.

processes that may have occurred long after the deposits were laid down. This is a key distinction when investigating the origin of the hematite and whether or not it is related to the origin of the layered deposits. In the following sections we describe hypotheses regarding formation of the hematite deposits and examine the plausibility of each mechanism in terms of consistencies and inconsistencies in our analysis of the data (Table 2). It is not our intention to duplicate previous discussions, rather to complement them, utilizing our detailed geomorphic mapping for regional context and timing constraints as well as recent MGS data (including new MOC images and higher-resolution MOLA and TES-derived data).

### 4.2. Primary Formation Mechanisms of Hematite

[23] Formation in a lake or sea environment has emerged as one of the leading hypotheses for the TM, Aram Chaos, and Valles Marineris hematite exposures. *Christensen et al.* [2000, 2001] advocated this mechanism based on geologic and topographic evidence. All hematite deposits are in situ and exhibit close associations with horizontal, friable, layered deposits. The Aram Chaos hematite deposit occurs in an impact basin that includes chaotic and outflow channel materials that are thought to be evidence of past release of groundwater [*Carr*, 1979; *Baker*, 1982], although other hypotheses such as $CO_2$-driven flows have been proposed [*Hoffman*, 2000].

[24] While formation of the friable deposits in a lake environment fits some of the data, there are major inconsistencies with this hypothesis. Analysis of MOLA data reveals that there is no obvious basin, at any scale, for the primary hematite deposit (Figure 7). For a subaqueous origin, the thickness of the layered materials indicate that a closed basin with at least 600 m of relief is required. The deposits are situated on a preexisting slope that was created by the end of the Noachian, uncharacteristic of a lacustrine environment (Figures 3, 4, and 7). This modern slope was produced by global-scale tilting from the ancient formation of the Tharsis rise, predominantly in the Noachian [*Phillips et al.*, 2001]. Late Noachian valley network azimuths follow the slope and are buried by, and therefore older than, the layered deposits and provide strong evidence that much of the Tharsis load must have been in place by the end of the Noachian (Figure 4) [*Hynek and Phillips*, 2001; *Phillips et al.*, 2001]. Additionally, an analysis of more than 25,000 western hemisphere faults is consistent with Tharsis, and

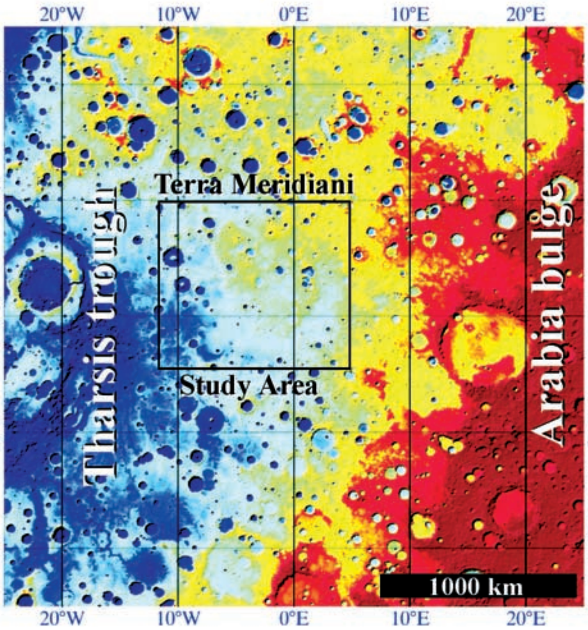


**Figure 7.** Regional shaded relief image of MOLA data centered on Terra Meridiani with a MOLA-based color scheme overlain. Warm colors signify high elevation and cool colors are low, with a total relief of ~5 km. Pole-to-pole topographic slope has been removed in data to emphasize regional variations in elevation [*Smith et al.*, 1999]. The Terra Meridiani deposits lie on a regional slope created from the ancient loading associated with the emplacement of the Tharsis rise [*Phillips et al.*, 2001]. It is unlikely that the younger TM materials are lacustrine in origin because of their emplacement on a pre-existing slope and lack of a >600 m closed basin at any scale.

therefore the slope, being present in the Noachian [*Anderson et al.*, 2001]. Sparse evidence for recent tectonism, both from MOLA data and our geomorphic mapping, suggests the current topography does reflect, to first order, the topography at the time of emplacement of the deposits. Thus, we conclude it is unlikely there has been a major uplift that would remove or disguise a large basin.

[25] The timing of the hematite deposits is also at odds with a lacustrine origin. In TM, the layered deposits bury dissected cratered terrain (Figure 4) mapped as Late Noachian [*Hynek and Phillips*, 2001]. Hence, the TM deposits postdate the only evidence of water in the mapped region (valley networks), inconsistent with a lacustrine origin. This is in agreement with the relative crater age dating of these deposits (Table 1). The implied post-Noachian age of these deposits is likely after the proposed clement period on Mars [*Pepin*, 1994; *Phillips et al.*, 2001; *Jakosky and Phillips*, 2001], evidence backed by global geomorphic analyses and geochemical analyses of Martian meteorites (for the summary, see *Jakosky and Phillips* [2001]). Although more recent climate perturbations have been hypothesized [*Baker et al.*, 1991], these brief episodes could not likely have produced long-lived "warm and wet" conditions necessary for the deposition of 600 m of lakebeds.

[26] Additionally, there are mineralogic inconsistencies with deposition in a lacustrine environment. A lacustrine environment should have precipitated other minerals in additional to the hematite. Previous interpretations of the Martian hematite have been compared to terrestrial BIF [*Christensen et al.*, 2000, 2001]. Yet no silica phase has been identified on Mars [*Bandfield et al.*, 2000], as is typically associated with terrestrial BIF [*Guilbert and Park*, 1986]. This suggests that Martian hematite formed by a different method than terrestrial BIF. In addition, evaporite deposits have not been identified from TES spectra in any section of the 600-m-thick layered sequence [*Bandfield et al.*, 2000], as would be expected from lacustrine deposition and eventual evaporation.

[27] Thermal oxidation of volcanic deposits is the other major category of primary hematite formation mechanisms. Cooling of Fe-rich volcanic material on Earth can result in lava flows, ignimbrites (ash flows of pyroclastic origin), and air fall material that are rich in hematite and magnetite; one of the best examples being the Tertiary volcanic deposits of El Laco, Chile as first described by *Park* [1961]. This formation process does not require abundant water at the time of emplacement and thus clement conditions after the Noachian epoch are not necessary. TES results suggesting a primarily andesitic–basaltic composition with 10–15% hematite (and lack of any carbonates or sulfur-bearing minerals above the ~10% detection limit) are more consistent mineralogically with a volcanic origin for the hematite deposits. However, there is a distinct lack of any sizable volcanic constructs in the TM region.

[28] We consider three broad categories of volcanic deposits—lava flows, ignimbrites, and air fall—and test their compatibility with the morphology, bedding characteristics, thickness and areal extent, erosional nature, and possible source region of the hematite and associated deposits. Lava flows have formed vast (>$10^6$ km$^2$) plains on Earth, Mars, and Venus [*Felder and Wilson*, 1975; *Greeley and Spudis*, 1981; *Tanaka*, 1986; *Head and Coffin*, 1997], comparable in size to the largest Martian hematite deposit. It is also possible that repeated flows could build up a layered sequence and variations in the lava's chemistry could produce hematitic and nonhematitic layers, as is seen at TM. The ridges that are observed in the etched terrain (E) (Figure 8A) may be remnants of volcanic vents or dikes and some MOC NA images of etched material exhibit possible primary volcanic features including flow lobes and compression ridges. However, in TM, few sizable features can uniquely be identified as source vents that would have contributed to the vast volume of materials. Additionally, many of the upper layers are extremely friable and have been intensely sculpted by aeolian processes (Figures 3A, 3C, 5, and 8A), which is inconsistent with an interpretation of competent lava beds. It is possible that the lower units are resistant lavas and the upper layered stacks consist of volcaniclastic materials.

[29] Thermal oxidation of ignimbrites is a potential explanation for the Martian hematite. The erosional characteristics of the fine-grained friable layered deposits are reminiscent of terrestrial ash flows. Variation in the competency of layered units may reflect different degrees of welding of volcanic ash units. However, terrestrial ignim-

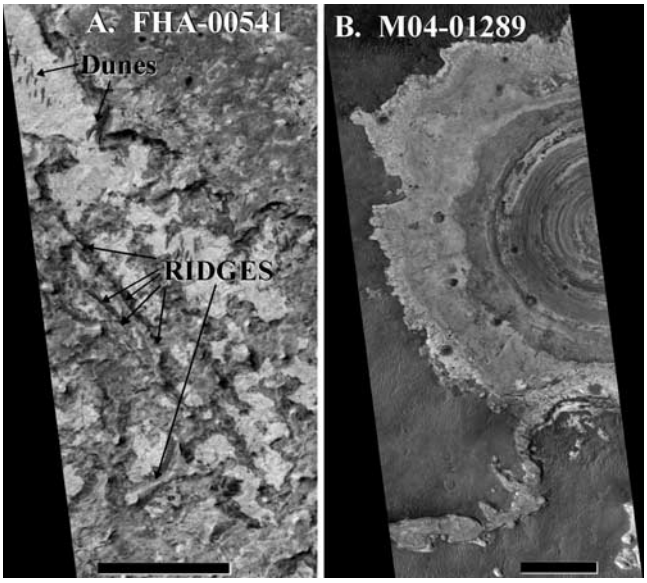


**Figure 8.** MOC NA images showing differential erosion of etched unit that may be related to cementation along joints and bedding planes from subsurface fluids. (A) Illustrates resistant linear ridges common to the etched unit that may represent areas where groundwater cemented particles along vertical joints. Alternatively, these features may be volcanic ridge vents or dikes. (B) Shows what may be vestiges of an eroded hydrothermal system. The presence of sand dunes, and not boulders, indicate the fine-grained nature of the materials. Scale bars are 1 km.

brites generally do not conform to preexisting topography and typically lack parallel bedding with significant topography [*Wilson and Houghton*, 2000], although repeated flow events could produce stratification. In contrast, the hematite deposit in TM conforms to the preexisting topography of the sloping cratered uplands that underlie the materials (Figure 3) and have parallel strata on the smallest observable scales. Moreover, few, if any, appreciable source vents for the ash flows are evident in the TM region.

[30] The final primary volcanic hypothesis is deposition of air fall from repeated episodes of explosive volcanism. Terrestrial air fall material from a single explosive event has been mapped over at least $10^7$ km$^2$ [*Froggatt et al.*, 1986] and repeated episodes of explosive volcanism can produce thick accumulations of ash fall deposits. The TM materials resemble air fall deposit characteristics [*Houghton et al.*, 2000] in that they are: 1) thin, parallel bedded deposits that conform to preexisting topography, 2) in most cases, extremely friable, and 3) are composed of small particles. One explanation for the presence of hematite is a change in eruption chemistry to an immiscible magnetite-rich magma that was altered to hematite upon cooling. Alternatively, Fe-rich ash could have been laid down and later oxidized to hematite through fluid flow. It is likely that Mars exhibited explosive volcanism in the past [*Reimers and Komar*, 1979; *Greeley and Spudis*, 1981; *Mouginis-Mark et al.*, 1982; *Greeley and Crown*, 1990; *Wilson and Head*, 1994] and when considering the bulk composition of the planet [*Lodders and Fegley*, 1997], it is plausible that eruptions produced Fe-rich ash deposits. Thus, thinly layered, fine-grained mantling deposits of ash that mimic preexisting topography could have been emplaced by repeated volcanic eruptions.

[31] Eruption of magnetite lava and ash has been documented on Earth and alteration of the magnetite to hematite is common in these units. El Laco, Chile, may be the best terrestrial example of extrusive pyroclastic eruptions of Fe-rich melt that resulted in the formation of numerous layers of lava, tuff, and air fall rich in hematite [*Park*, 1961; *Rogers*, 1968; *Guilbert and Park*, 1986; *Nyström and Henríquez*, 1994]. The hematite is believed to have replaced magnetite in an oxidation reaction during cooling. Cerro de Mercado, Durango, Mexico, is another Fe-rich suite of extrusive volcanic deposits. Explosive eruptions of Fe-rich magma produced stratiform layers of hematite-magnetite-apatite tuffs, pyroclastics, agglomerates, flows, and dikes [*Swanson et al.*, 1978]. Multiple layers of hematite ash are found within the deposits and may be analogous to Martian hematite.

[32] *Catling and Moore* [2001] have argued that thermal oxidation of volcanic deposits on Mars is untenable due to the low oxygen fugacity derived from analyses of mafic and ultramafic Martian meteorites. However, atmospheric conditions were different in the past and there are no known Martian meteorites from the Early Hesperian period when the hematite-rich layered deposits likely formed. Moreover, the TM region exhibits an intermediate composition [*Bandfield et al.*, 2000] that is not represented by the mafic and ultramafic meteorites. The andesitic composition found in TM may have had an adequate oxygen fugacity and water content in the magma to produce primary hematite from volcanic eruptions [*Chapman and Tanaka*, 2002].

[33] If these deposits are volcanic ash, there must have been a source or sources of the $>1 \times 10^5$ km$^3$ of mantling deposits. This is a conservative estimate, using MOLA data, to determine the volume of the superposed friable deposits ($P_1$, $P_2$, $P_3$, E, I) that encompass an area of $3.13 \times 10^5$ km$^2$. The primary argument against a volcanic origin of Martian hematite is a lack of nearby sources [*Christensen et al.*, 2000, 2001]. Theoretical arguments indicate that the reduced gravity and atmospheric drag on Mars should result in a broad distribution of pyroclastic materials; much more so than on Earth [*Wilson and Head*, 1981a, 1981b, 1994; *Hynek et al.*, 2002]. Thus, a lack of local sources does not preclude this hypothesis. There is evidence that these deposits were once much greater in extent as exhibited in outliers in cratered units of the TM region (see section 3 and Figure 2). Nearby craters with layered stacks of material within them may have originally been laterally continuous with the ~600-m-thick stack of layered materials that host the hematite. *Malin and Edgett* [2000] indicated that similar layered deposits are found in equatorial regions globally and that most of these deposits probably formed by a similar mechanism, consistent with previous work by *Schultz and Lutz* [1988]. In fact, the unit types and the general aspects of the stratigraphic sequence are repeated in different locations and geologic settings separated by thousands of kilometers [*Malin and Edgett*, 2000]. *Hynek et al.* [2002] used MOC and MOLA data to test the hypothesis that these materials may be genetically linked to one or more source regions. The workers found that these deposits are morphologically similar to pyroclastics and that there is a general thickening

of deposits in the direction of the Tharsis region. These observations led them to hypothesize that the friable layered materials that host the hematite could be remnants of large-scale ash deposits from repetitive explosive eruptions in the Tharsis region. We conclude it is plausible that the friable layered equatorial deposits could have come from explosive eruptions of distal volcanoes. Hematite may have formed as Fe-rich deposits that were oxidized upon eruption and cooling or by a later secondary mechanism in the preexisting ash beds.

### 4.3. Secondary Formation Mechanisms of Hematite

[34] Hematite has been documented to develop from secondary processes involving preexisting strata. On Earth, hydrothermal alteration of Fe-rich ignimbrites or air fall can result in the oxidation of magnetite to hematite [*Hauck*, 1990; *Hitzman et al.*, 1992]. In fact, tabular concordant bodies of hematite can originate from movement of hydrothermal fluids between poorly welded tuff units [*Hitzman et al.*, 1992]. There is ample evidence for subsurface water and volcanism over Martian history [*Greeley and Spudis*, 1981; *Baker*, 1982; *Tanaka*, 1986; *Carr*, 1996; *Baker*, 2001]. Thus, it is likely that hydrothermal systems have operated throughout much of Mars' history and may still be occurring at present [*Sakimoto*, 2001]. There is evidence for post-Noachian groundwater processes in proximity to all three hematite locales raising the possibility that subsurface water may have been involved in hematite genesis (Figure 1). A majority of all known outflow channels on Mars are found in the region east of the Tharsis Montes. These features have been compared to catastrophic flooding on Earth and are often interpreted to be the result of confined groundwater release from breaching of an aquifer [*Carr*, 1979; *Baker*, 1982]. *Masursky et al.* [1986] proposed that magmatic heating could locally melt ice in the Martian regolith, causing the release of copious amounts of water. The outflow channels were active during most of the Hesperian [*Rotto and Tanaka*, 1995] and are seen fingering between the Terra Meridiani, Aram Chaos, and Valles Marineris hematite deposits (Figure 1). While there are no outflow channels within the TM deposits, these materials are immediately upgradient from Iani Chaos and the outflow channels Ares and Mawrth Valles. It is likely that the enormous volumes of subsurface water required to carve the outflow channels were not only located in the discrete places where the channels originated. More probable, there was a regional water table in this area during portions of the Hesperian that could have been responsible for formation of the hematite. A water-rich substrate in this area of Mars may have been a relic from extensive regional fluvial denudation in the Late Noachian [*Hynek and Phillips*, 2001]. As discussed in section 2.3 above, we have determined from mapping relations that the hematite deposit in TM postdates Late Noachian dissected terrain and crater density determinations indicate a possible age of Early Hesperian. This argues that the hematite plain in TM formed shortly before, or possibly coeval, with outflow channels and that during middle Martian history there were active groundwater processes east of the Tharsis rise. The proximity and likely ages of the three hematite deposits and nearby outflow channels may be more than coincidental. Hematite may have only formed in this region because it is intimately linked to magmatic heating, groundwater circulation, and catastrophic release of water. Numerous MOC images in the etched terrain (E) show differential erosion in the form of resistant ridges and mesas (Figure 8A). These may represent cementing along joints and weak bedding planes from groundwater flow. Additionally, a circular ringed structure is seen in two MOC images west of TM, and may be the vestige of a hydrothermal system (Figure 8B). This feature is reminiscent of aerial photographs of ringed geyser basins and other hydrothermal constructs on Earth. However, high-resolution mineralogical data from future missions are necessary for a unique interpretation. Hematite in TM formed along a single stratigraphic horizon and did not form throughout the TM layered deposits. This may reflect a differing starting composition of the hematite-rich layer (presumably more Fe-rich) or a weak bedding plane where hydrothermal deposition could occur.

[35] There are inconsistencies with a hydrothermal origin for the Martian hematite, including an absence (within the detection limits of TES) of any minerals that are typically found in association with terrestrial hematite formed hydrothermally. Results from TES show no evidence of sulfur-based minerals in any of the hematite locales. The hematite sites are associated with outflow channels but this is not necessarily an indication of magmatic activity. Other mechanisms have been hypothesized for the formation of the outflow channels that require no heating [e.g., *Carr*, 1979; *Hoffman*, 2000]. In TM, our mapping revealed no structural modifications of the layered sequence since deposition, which might be expected from a nearby magmatic source.

[36] Groundwater diagenesis is a well-documented secondary formation mechanism of hematitic soils (laterites) on Earth [e.g., *McFarlane*, 1976]. In this scenario, the slow movement of acidic groundwater can result in the dissolution of mafic minerals. A $CO_2$-dominated Martian atmosphere would result in groundwater rich in bicarbonate, facilitating the dissolution of iron in mafic rocks [*Catling and Moore*, 2001]. The ions may then be transported and precipitated in a higher pH and Eh environment, forming crystalline hematite. On Earth, transportation of metals is often associated with, although not limited to, vertical flux of the groundwater table [*McFarlane*, 1976]. Laterites exist on flat or nearly flat surfaces and are the only terrestrial hematite occurrences that rival the areal magnitude of the Martian hematite. The loose association of hematite with outflow channels may be indicative of an active groundwater system during or shortly after emplacement of the friable layered deposits that contain hematite. Nearby magmatic heating may have created a persisting low-temperature groundwater system in the hematite-rich units. The flux of this aquifer (presumably from magmatism) may be analogous to the rising and falling of water tables on Earth that produce hematite-bearing laterite deposits. Hence, it may be possible to have a relatively long-lived active groundwater system in this region under present climatic conditions. Aforementioned MOC images (Figures 8A and 8B) show evidence of aqueous cementation, possibly under low-temperature conditions.

[37] On Earth, laterite formation is inherently coupled to climate and is formed almost exclusively in tropical or subtropical climates averaging >1200 mm of precipitation per year [*Price et al.*, 1997]. There are no indications of

precipitation and surface runoff at the time of hematite emplacement, which was probably formed after the proposed clement period of Mars. Additionally, groundwater diagenesis typically results in the formation of red, not gray, hematite on Earth (although burial metamorphism may have altered Martian hematite from red to gray [*Lane et al.*, 2002]). Laterites usually have diffuse boundaries whereas the Martian hematite has a sharp correlation with rock units, an observation that *Christensen et al.* [2000, 2001] used to argue against this formation mechanism. However, this could be a result of the extensive erosion and wind-transport of sediment; under such conditions, sharp correlation along erosional contacts might be expected.

## 5. Discussion

[38] Hematite on Mars is found in close association with thinly bedded materials susceptible to erosion. TM and the two minor occurrences are all within 80 degrees of longitude of each other and reside less than 10 degrees from the equator. Viking IRTM data and TES data [*Kieffer et al.*, 1977; *Presley and Christensen*, 1997; *Jakosky and Mellon*, 2001] suggest that the layered deposits are composed of submillimeter material. MOC images reveal a lack of boulders near geologic contacts (Figures 5 and 8A), consistent with a composition of small particles. Imagery of the thinly layered TM units indicates that they were likely emplaced episodically over time. There is a great range of competencies within layers as is evident from the slope- to cliff-forming morphologies along contacts. In TM, the layered materials appear to have once been much more extensive and many outliers are present. Mapping relations and crater counts reveal that the TM deposits likely formed in the Late Noachian to Early Hesperian time period of Mars, although a precise age is impossible given the history of burial and exhumation. The origin of the layered materials is probably volcanic, in the form of ash falls and/or flows, though some of the lower layers exhibit possible effusive lava flow features. No major volcanic constructs have been identified in TM although source regions may remain buried. If the material is volcanic air fall, the source(s) may be several thousand kilometers away [*Hynek et al.*, 2002].

[39] On Earth, hematite can form in many diverse ways including chemical precipitation from an ambient subaqueous environment or via eruption of an immiscible Fe-rich magma. Formation may occur in a primary setting or as a secondary mineralization and often, although not always, requires water. Our regional analysis aids in scrutiny of the possible origin mechanisms. Formation from chemical precipitation in a paleolake environment is unlikely because of the lack of a topographic basin and mineralogic and timing inconsistencies. Thermal oxidation of volcanic deposits is the other major formation mechanism of primary hematite and remains a viable hypothesis. The interpretation of volcanic air fall or ash flow is consistent with the friable fine-grained layered materials in which the hematite resides. There are few identified volcanic source vents in regions of hematite, however distal eruptions of thermally oxidized volcanic ash cannot be ruled out. In this scenario, a wide dispersion of hematitic ash is expected but not observed in TES data. This result may be due to some deposits being still buried, extensive erosion of the layered deposits, or minor concentrations of hematite escaping detection by TES. The circulation of hydrothermal fluids in the preexisting, layered, Fe-rich strata is the formation mechanism of secondary hematite that is most consistent with observations. Large concordant bodies of hematite can form in this manner on Earth as a result of fluid flow along contacts of poorly welded tuffs [*Hitzman et al.*, 1992]. All three locales are in close proximity to features probably carved by release of groundwater near the time period when the hematite likely formed. Emplacement of pyroclastics (and possibly effusive lavas) from repeated eruptions and subsequent formation of hematite through precipitation from Fe-rich fluid along tuff units is the most consistent hypothesis in terms of regional geologic, topographic, and spectral observations.

[40] **Acknowledgments.** This research was supported by NASA Planetary Geology and Geophysics Grant NAG5-7830, an MDAP Grant NAG5-11202, and by Contract Number 39361-6452 from Cornell University as part of the Athena Team work. We thank Steve Hauck II, Melissa Lane, and an anonymous reviewer for their thoughtful suggestions and Frank Seelos IV for aid in mosaic generation.

## References

Allen, C. C., F. Westall, and R. T. Schelble, Importance of a martian hematite site for astrobiology, *Astrobiology*, *1*, 111–123, 2001.
Anderson, R. C., J. M. Dohm, M. P. Golombek, A. F. C. Haldemann, B. J. Franklin, K. L. Tanaka, J. Lias, and B. Peer, Primary centers and secondary concentrations of tectonic activity through time in the western hemisphere of Mars, *J. Geophys. Res.*, *106*, 20,563–20,585, 2001.
Arvidson, R. E., et al., Standard techniques for presentation and analysis of crater size-frequency data, *Icarus*, *37*, 467–474, 1979.
Arvidson, R. E., K. S. Deal, B. M. Hynek, F. P. Seelos IV, N. O. Snider, M. T. Mellon, and J. B. Garvin, Thermal inertia, albedo, and MOLA-derived roughness for terrains in the Terra Meridiani area, Mars, *Lunar Planet. Sci.* [CD-ROM], *XXXIII*, abstract 1748, 2002.
Baker, V. R., *The Channels of Mars*, Univ. of Tex. Press, Austin, 1982.
Baker, V. R., Water and the martian landscape, *Nature*, *412*, 228–236, 2001.
Baker, V. R., R. G. Strom, V. C. Gulick, J. S. Kargel, G. Komatsu, and V. S. Kale, Ancient oceans, ice sheets, and the hydrological cycle on Mars, *Nature*, *352*, 589–594, 1991.
Bandfield, J. L., V. E. Hamilton, and P. R. Christensen, A global view of martian surface compositions from MGS-TES, *Science*, *287*, 1626–1630, 2000.
Barlow, N. G., Crater size–frequency distribution and a revised martian chronology, *Icarus*, *75*, 285–305, 1988.
Carr, M. H., Formation of martian flood features by release of water from confined aquifers, *J. Geophys. Res.*, *84*, 2995–3007, 1979.
Carr, M. H., *Water on Mars*, Oxford Univ. Press, New York, 1996.
Catling, D. C., and J. M. Moore, Sedimentary hematite on Mars and its implications for the early martian environment, *Lunar Planet. Sci.*, [CD-ROM], *XXXII*, abstract 2053, 2001.
Chapman, M. G., and K. L. Tanaka, Related magma–ice interactions: Possible origins of chasmata, chaos and surface materials in Xanthe, Margaritifer, and Meridiani Terrae, Mars, *Icarus*, *155*, 324–339, 2002.
Christensen, P. R., et al., Detection of crystalline hematite mineralization on Mars by the Thermal Emission Spectrometer: Evidence for near-surface water, *J. Geophys. Res.*, *105*, 9623–9642, 2000.
Christensen, P. R., R. V. Morris, M. D. Lane, J. L. Bandfield, and M. C. Malin, Global mapping of martian hematite mineral deposits: Remnants of water-driven processes on early Mars, *J. Geophys. Res.*, *106*, 23,873–23,886, 2001.
Edgett, K. S., and T. J. Parker, Water on early Mars: Possible subaqueous sedimentary deposits covering ancient cratered terrain in western Arabia and Sinus Meridiani, *Geophys. Res. Lett.*, *24*, 2897–2900, 1997.
Felder, G., and L. Wilson, *Volcanoes of the Earth, Moon, and Mars*, Elek Sci., London, 1975.
Froggatt, P. C., C. S. Nelson, L. Carter, G. Griggs, and K. P. Black, An exceptionally large late Quaternary eruption from New Zealand, *Nature*, *319*, 578–582, 1986.
Golombek, M., et al., Downselection of landing sites for the Mars Exploration Rovers, *Lunar Planet. Sci.*, [CD-ROM], *XXXIII*, abstract 1234, 2002.
Greeley, R., and D. A. Crown, Volcanic geology of Tyrrhena Patera, Mars, *J. Geophys. Res.*, *95*, 7133–7149, 1990.

Greeley, R., and P. Spudis, Volcanism on Mars, *Rev. Geophys. Space Phys.*, *19*, 13–41, 1981.
Guilbert, J. M., and C. F. Park Jr., *The Geology of Ore Deposits*, W. H. Freeman, New York, 1986.
Hartmann, W. K., and G. Neukum, Cratering chronology and the evolution of Mars, *Space Sci. Rev.*, *96*, 165–194, 2001.
Hartmann, W. K., J. Anguita, M. A. de la Casa, D. C. Berman, and E. V. Ryan, Martian cratering, 7, The role of impact gardening, *Icarus*, *149*, 37–53, 2001.
Hauck, S. A., Petrogenesis and tectonic setting of Middle Proterozoic iron-oxide-rich ore deposits—An ore deposit model for Olympic Dam-type mineralization, *U. S. Geol. Surv. Bull.*, *1932*, 4–39, 1990.
Head, J. W., III, and M. F. Coffin, Large igneous provinces: A planetary perspective, in *Large Igneous Provinces: Continental, Oceanic, and Planetary Flood Volcanism*, pp. 411–438, AGU, Washington, D. C., 1997.
Hitzman, M. W., N. Oreskes, and M. T. Einaudi, Geological characteristics and tectonic setting of Proterozoic iron oxide (Cu-U-Au-REE) deposits, *Precambrian Res.*, *58*, 241–287, 1992.
Hoffman, N., White Mars: A new model for Mars' surface and atmosphere based on $CO_2$, *Icarus*, *146*, 326–342, 2000.
Houghton, B. F., C. J. N. Wilson, and D. M. Pyle, Pyroclastic fall deposits, in *Encyclopedia of Volcanoes*, pp. 555–570, Academic, San Diego, Calif., 2000.
Hynek, B. M., and R. J. Phillips, Evidence for extensive denudation of the martian highlands, *Geology*, *29*, 407–410, 2001.
Hynek, B. M., R. E. Arvidson, and R. J. Phillips, Preliminary stratigraphy of Terra Meridiani, Mars, *Lunar Planet. Sci.*, [CD-ROM], *XXXII*, abstract 1179, 2001.
Hynek, B. M., R. E. Arvidson, and R. J. Phillips, Explosive volcanism from Tharsis: Global evidence in the martian geologic record, *Lunar Planet. Sci.*, [CD-ROM], *XXXIII*, abstract 1408, 2002.
Jakosky, B. M., and M. T. Mellon, High-resolution thermal inertia mapping of Mars: Sites of exobiological interest, *J. Geophys. Res.*, *106*, 23,887–23,908, 2001.
Jakosky, B. M., and R. J. Phillips, Mars' volatile and climate history, *Nature*, *412*, 237–244, 2001.
Kieffer, H. H., T. Z. Martin, A. R. Peterfreund, B. M. Jakosky, E. D. Miner, and F. D. Palluconi, Thermal and albedo mapping of Mars during the Viking primary mission, *J. Geophys. Res.*, *82*, 4249–4291, 1977.
Lane, M. D., R. V. Morris, S. A. Mertzman, and P. R. Christensen, Evidence for platy hematite grains in Sinus Meridiani, Mars, *J. Geophys. Res.*, *107*, doi:10.1029/2001JE001832, in press, 2002.
Lodders, K., and B. Fegley Jr., *The Planetary Scientist's Companion*, Oxford Univ. Press, New York, 1997.
Lyons, J. L., Jr., and S. E. Clabaugh, Pryoclastic and extrusive iron ore at Durango, Mexico, *Econ. Geol.*, *68*, 1216–1217, 1973.
Malin, M. C., and K. S. Edgett, Sedimentary rocks of early Mars, *Science*, *290*, 1927–1937, 2000.
Malin, M. C., and K. S. Edgett, The Mars Global Surveyor Mars Orbiter Camera: Interplanetary cruise through primary mission, *J. Geophys. Res.*, *106*, 23,429–23,570, 2001.
Masursky, H., M. G. Chapman, A. L. Dial Jr., and M. E. Strobell, Episodic channeling punctuated by volcanic flows in Mangala Valles region, Mars (abstract), *NASA Tech. Memo. 88383*, pp. 459–461, 1986.
McFarlane, M. J., *Laterite and Landscape*, Academic, San Diego, Calif., 1976.
Mouginis-Mark, P. J., L. Wilson, and J. W. Head III, Explosive volcanism of Hecates Tholus, Mars: Investigation of eruption conditions, *J. Geophys. Res.*, *87*, 9890–9904, 1982.
Nyström, J. O., and F. Henríquez, Magmatic features of iron ores of the Kiruna type in Chile and Sweden: Ore textures and magnetite geochemistry, *Econ. Geol.*, *89*, 820–839, 1994.
Park, C. F., Jr., A magnetite "flow" in northern Chile, *Econ. Geol.*, *56*, 431–436, 1961.
Pepin, R. O., Evolution of the martian atmosphere, *Icarus*, *111*, 289–304, 1994.
Phillips, R. J., et al., Ancient geodynamics and global-scale hydrology of Mars, *Science*, *291*, 2587–2591, 2001.
Presley, M. A., The origin and history of surficial deposits in the central equatorial region of Mars, M.A. thesis, Wash. Univ., St. Louis, Missour., 1986.
Presley, M. A., and R. E. Arvidson, Nature and origin of materials exposed in the Oxia Palus–western Arabia–Sinus Meridiani region, Mars, *Icarus*, *75*, 499–517, 1988.
Presley, M. A., and P. R. Christensen, Thermal conductivity measurements of particulate materials, 2, Results, *J. Geophys. Res.*, *102*, 6551–6566, 1997.
Price, G. D., P. J. Valdes, and B. W. Sellwood, Prediction of modern bauxite occurrence; implications for climate reconstruction, *Paleogeogr. Paleoclimatol. Paleoecol.*, *131*, 1–13, 1997.
Reimers, C. E., and P. D. Komar, Evidence for explosive volcanic density currents on certain martian volcanoes, *Icarus*, *39*, 88–110, 1979.
Rogers, D. P., The extrusive iron oxide deposits, "El Laco," Chile, *Econ. Geol.*, *63*, 700, 1968.
Rotto, S., and K. L. Tanaka, Geologic/geomorphic map of the Chryse Planitia region of Mars, *U.S. Geol. Surv. Misc. Invest. Map, I-2441*, 1995.
Sakimoto, S. E. H., Geologically recent martian volcanism and flooding in Elysium Planitia and Ceberus Rupes: Plains-style eruptions and related water release?, *Geol. Soc. Am. Abstr. Programs*, *33*(6), A431–A432, abstract 25349, 2001.
Schultz, P. H., and A. B. Lutz, Polar wandering of Mars, *Icarus*, *73*, 91–141, 1988.
Scott, D. H., and K. L. Tanaka, Geologic map of the western equatorial region of Mars, *U.S. Geol. Surv. Misc. Invest. Map, I-1802-A*, 1986.
Smith, D. E., et al., The global topography of Mars and implications for surface evolution, *Science*, *284*, 1495–1503, 1999.
Swanson, E. R., R. P. Keizer, J. L. Lyons, and S. E. Clabaugh, Tertiary volcanism and caldera development near Durango City, Sierra Madre Occidental, Mexico, *Geol. Soc. Am. Bull.*, *89*, 1000–1012, 1978.
Tanaka, K. L., The stratigraphy of Mars, *Proc. Lunar Planet. Sci. Conf., XVIIth, J. Geophys. Res.*, *91*, E139–E158, 1986.
Wilson, C. J. N., and B. F. Houghton, Pyroclast transport and deposition, in *Encyclopedia of Volcanoes*, pp. 545–554, Academic, San Diego, Calif., 2000.
Wilson, L., and J. W. Head, Theoretical analysis of martian explosive eruption mechanisms, paper presented at Third International Colloquium on Mars, NASA/Div. of Planet. Sci. of Am. Astron. Soc./Lunar Planet. Inst., Pasadena, Calif., 1981a.
Wilson, L., and J. W. Head, Volcanic eruption mechanisms on Mars: Some theoretical constraints (abstract), *Proc. Lunar Planet. Sci. Conf., XIIth*, 1194–1196, 1981b.
Wilson, L., and J. W. Head, Mars: Review and analysis of volcanic eruption theory and relationships to observed landforms, *Rev. Geophys.*, *32*, 221–263, 1994.

R. E. Arvidson and R. J. Phillips, Earth and Planetary Sciences and McDonnell Center for the Space Sciences, Washington University, St. Louis, MO, USA.

B. M. Hynek, Earth and Planetary Sciences, Washington University, Campus Box 1169, St. Louis, MO 63130, USA. (hynek@levee.wustl.edu)